LEGIBILITY NOTICE

A major purpose of the Technical Information Center is to provide the broadest dissemination possible of information contained in DOE's Research and Development Reports to business, industry, the academic community, and federal, state and local governments.

Although a small portion of this report is not reproducible, it is being made available to expedite the availability of information on the research discussed herein.

1

LA-UR -87-3929

LA-UR--87-3929

DE88 003155

Los Alamos National Laboratory is operated by the University of California for the United States Department of Energy under contract W-7405-ENG-36

TITLE **MODE MEDIA INTERACTIONS IN AN FEL (Free Electron Laser)**

AUTHOR(S) **Steven J. Gitomer, Brian D. McVey, and Steven C. Bender**

SUBMITTED TO Proceedings of the Ninth Annual Free Electron Laser Conference
11-16 September 1987, Williamsburg Virginia

DISCLAIMER

MASTER

Los Alamos National Laboratory
Los Alamos New Mexico 87545

MODE MEDIA INTERACTIONS IN AN FEL *

S J Gitomer, S C Bender & B D McVey

Los Alamos National Laboratory

Los Alamos, NM 87545

ABSTRACT

It is well known that the e-beam gain and refractive properties in an FEL alters the optical mode behavior from that of a bare resonator We report here on 3-D simulations with FELEX [1] and experiments on the 10 6 micron wavelength Los Alamos FEL [2] performed to assess the importance of this effect for a range of e-beam parameters Two sets of measurements are made for a near concentric cavity with optical axis displaced from the electron beam axis The first is a static measurement made during cavity mode saturation of the optical beam centroid referred to each resonator mirror The optical detector scheme for this part of the experiment uses a 256 element integrating pyroelectric array The second is a dynamic measurement made during cavity mode decay of the motion of the optical beam centroid and waist referred to each resonator mirror The optical detection scheme for this part of the experiment consists of a three-part split mirror detector viewing two different optical paths These measurements quantify the gain and refractive properties of the electron beam when compared to FELEX simulations Implications for FEL alignment schemes and future high-power FELs will be discussed

*Work performed under the auspices of the United States Department of Energy,

and supported by the United States Army Strategic Defense Command

1 B D McVey, Nucl Instrum & Methods A250 449 (1986)

2 B E Newnam et al, IEEE J Quant Electron QE-21 867 (1985)

I INTRODUCTION

In this paper, we are concerned with the subject of mode-media interactions in FELs By the term "mode-media interactions" we mean the effects that the gain medium (i e e-beam traversing wiggler) has upon the optical mode within the laser cavity Effects of the medium upon the laser mode have been referred to over the years as thermal lensing, gain guiding, self-trapping and self-focusing for example The above all relate to effects which nonlinear index of refraction variations have upon laser beams In the case of an FEL, we concentrate our attention on the angular deviation the laser beam exhibits on passing through the wiggler while interacting with the e-beam In order to enhance this angular deviation in the Los Alamos FEL, we arrange the experiment so that the cavity optical axis may be offset relative to the axis of the uniform wiggler. Time integrated and time resolved measurements are made of the laser beam coupled out of the optical cavity for a range of offset choices. The data is analyzed to yield information on the angular deviation experienced by the laser beam as it traverses the wiggler

In the remainder of this paper, we discuss the results obtained from theoretical calculations with the 3-D simulation code FELEX [1] used to model the FEL for a range of optical axis offsets, e-beam emittances, e-beam energy spreads and peak currents We end with a discussion of the results and recommendations as to how to enhance the angular deviation and thus the observability of the mode-medium interaction

II THEORECTICAL RESULTS

The 3-D simulation code FELEX has been used to model the mode media interaction experiments The parameters at our disposal are many - however, we limited our study to variations of optical axis offset relative to wiggler axis (0 0 to 0 12 cm), e-beam emittance (2π and 3π mm mrad), e-beam energy spread (1% and 2%), and e-beam peak current (150 and 300 amps) A single wavelength FEL optical mode was simulated, the wavelength (typically 10 1 microns for our experimental parameters) being chosen to have the highest single pass small signal gain. The simulation runs were made beginning with a small optical signal injected into the uniform wiggler, propagating parallel to the e-beam The optical beam makes some tens to hundreds of passes until saturation is reached, at which time the e-beam is turned off and the optical mode decays In what follows we discuss the small signal gain and extraction efficiency, the saturated state of the optical mode with the e-beam turned on, and the oscillations of the optical mode width and the optical mode centroid after the e-beam is turned off

Let us first consider how the FEL behaves as measured by small signal gain and by extraction efficiency By small signal gain, we mean the ratio of electric field amplitude at the wiggler exit to the same quantity at the wiggler entrance The extraction efficiency is the fractional electron power which is converted to light Figure 1 shows the small signal gain plotted as a function of optical axis offset for the six different choices of e-beam parameters The plot shows that the small signal gain decreases with increasing optical axis offset The decrease is more pronounced for the "better" e-beam parameter choices ("better" meaning smaller emittance, smaller energy spread or higher peak current) As with the small signal gain, we plot extraction efficiency versus optical axis offset for the six

different sets of e-beam parameters in Fig 2 The extraction efficiency is seen to decrease (generally) with increasing optical axis offset The kinks or jumps seen in the lowest curve (for 3π mm mrad, 2% energy spread, 150 amp peak current) and the next higher curve (for 2πmm mrad, 2% energy spread, 150 amp peak current) are traced to a change in wavelength between the 0 03 cm (10 1 micron wavelength) and 0.06 cm (10.2 micron wavelength) offset runs The pronounced sensitivity of extraction efficiency to choice of wavelength is thus demonstrated

The optical mode reaches saturation in some tens to hundreds of passes through the cavity The mode medium interaction can be readily seen in the skewing of the optical cavity mode centroid, that is, the deviation of the optical beam from parallel propagation Stated in another way, the optical beam enters the wiggler at an angle α to the cavity axis The optical beam exits the wiggler making an angle γ to the cavity axis The skewing is just $\gamma - \alpha$ This quantity is referred to as the bend angle of the optical mode The optical beam returns to the back reflecting mirror making an angle β with the optical cavity axis This angle is referred to as the tilt angle The results of our simulations are displayed in Fig 3 In these figures, we plot the optical mode centroid measured at the optical cavity mirrors as a function of the optical axis offset The optical mode centroid at the mirrors is an experimentally accessible quantity Results for 2π mm mrad emittance appear in Figs 3A-3C and results for 3π mm mrad emittance are given in Figs 3D-3F The figures show that the optical mode centroid exhibits greater skewing with greater offset Error bars denote oscillation limits of the optical mode centroid The dashed line in the figures is a 1-to-1 indicator Thus, the skewing is seen to be greater at the right

(outcoupling) mirror than at the left (backreflecting) mirror and greater for 2π than for 3π mm mrad emittance choice In general, greater skewing obtains with "better" e-beam parameters

In Fig 4, we give a composite of the bend and tilt angles taken directly from the code results, as defined above. In the figure, these angles are plotted as a function of the optical axis offset for the six sets of parameter choices. Notice that for the 2π mm mrad emittance runs, the vertical axis scale covers twice the range as for the 3π mm mrad emittance runs As in the case of figure 3, a vertical range is given in a case in which the plotted quantity still oscillated about an average value by the time the e-beam was turned off Again we see that the values of the angles increase with increasing offset and increase for "better" choices of e-beam parameters

After the FEL has reached saturation, the e-beam is turned off The optical cavity mode now begins to oscillate about the empty cavity mode and to decay (ringdown) One measure of the mode medium interaction is how large an oscillation can be seen in the cavity mode width This oscillation of the optical mode width with time has been given the anthropomorphic designation of a "breathing mode " In Fig 5, we show results for the range of this breathing mode oscillation for the six parameter choices quoted above What is plotted is optical mode width versus optical axis offset There appears to be no systematic dependence of oscillation range on optical axis offset The largest range of oscillation observed in the simulations is found for 2π mm mrad emittance, 1% energy spread and 150 amps peak e-beam current

Another measure of the mode medium interaction is how large an oscillation can be observed in the optical cavity mode centroid. This oscillation, often referred to as a "walking mode," arises because, as shown in Fig 3, during the e-beam pulse the optical mode centroid deviates from the 1-to-1 line. The 1-to-1 line defines the optical axis in the absence of the e-beam In Fig. 6, we present plots of the range of oscillation of the optical beam centroid as a function of the cavity axis offset for the six e-beam parameter choices quoted above. For the walking mode oscillation, we see that there is a pronounced dependence upon offset for a given emittance We also note that the "better" the e-beam parameters, the greater the walking mode oscillation

III CONCLUSIONS

We have seen that by varying a number of optical cavity and e-beam parameters a number of effects are observed in (1) small signal gain, (2) extraction efficiency, (3) bend and tilt angles, (4) breathing mode amplitude and (5) walking mode amplitude The various effects can be summarized best in TABLE I With an up-arrow indicating increase and a down-arrow decrease, we see that, for example, an increase in emittance (ϵ) leads to a decrease in breathing mode amplitude or an increase in peak current leads to an increase in tilt angle If we wish to enhance the mode medium interaction manifestation, TABLE I suggests that we decrease emittance, decrease energy spread and increase peak current If we wish to enhance the observability of the breathing mode, it is more useful to decrease energy spread of the e-beam than it is to increase the e-beam peak current

FIGURE CAPTIONS

Figure 1 Small signal gain vs optical axis offset Curves are labelled with e-beam emittance (mm mrad), e-beam energy spread (percent) and e-beam peak current (amps).

Figure 2 Extraction efficiency vs optical axis offset. Curves are labelled with e-beam emittance (mm mrad), e-beam energy spread (percent) and e-beam peak current (amps)

Figure 3 Optical beam centroid vs optical axis offset Results shown for both optical cavity mirrors and for a range of e-beam parameters: emittance of 2 π mm mrad and 1% or 2% energy spread and 150 amps or 300 amps peak current in figures (a)-(c); emittance of 3 π mm mrad and 1% or 2% energy spread and 150 amps or 300 amps peak current in figures (d)-(f).

Figure 4 Bend angle ($\gamma - \alpha$) and tilt angle (β) vs optical axis offset. Results shown for a range of e-beam parameters emittance of 2 π mm mrad and 1% or 2% energy spread and 150 amps or 300 amps peak current in figures (a)-(c); emittance of 3 π mm mrad and 1% or 2% energy spread and 150 amps or 300 amps peak current in figures (d)-(f)

Figure 5 Optical mode width vs optical axis offset Results shown are taken during the decay of the optical mode, following

turn-off of the e-beam for a range of e-beam parameters emittance of 2 π mm mrad and 1% or 2% energy spread and 150 amps or 300 amps peak current in figures (a)-(c), emittance of 3 π mm mrad and 1% or 2% energy spread and 150 amps or 300 amps peak current in figures (d)-(f).

Figure 6 Optical mode centroid (measured at outcoupler mirror) vs. optical axis offset Results shown are taken during the decay of the optical mode, following turn-off of the e-beam for a range of e-beam parameters· emittance of 2 π mm mrad and 1% or 2% energy spread and 150 amps or 300 amps peak current in figures (a)-(c), emittance of 3 π mm mrad and 1% or 2% energy spread and 150 amps or 300 amps peak current in figures (d)-(f)

EXPERIMENTAL PARAMETERS (↑)	Offset	Emittance	Energy Spread	Current
RESULTS				
1. Small signal gain	↓	↓	↓	↑
2. Extraction efficiency	↓	both	both	↑
3. Saturated mode angles				
a. Bend angle	↑	↓	↓	↑
b. Tilt angle	↑	↓	↓	↑
4. Breathing mode amplitude ..	flat	↓	↓	flat*
5. Walking mode amplitude ...	↑	↓	↓	flat*

TABLE I. Summary of theoretical results for four experimental quantities which were varied. An up arrow denotes an increase while a down arrow denotes a decrease of the listed result for an assumed increase of the experimental parameter. Flat denotes no change or possibly a slight increase while both denotes no definite conclusion.*

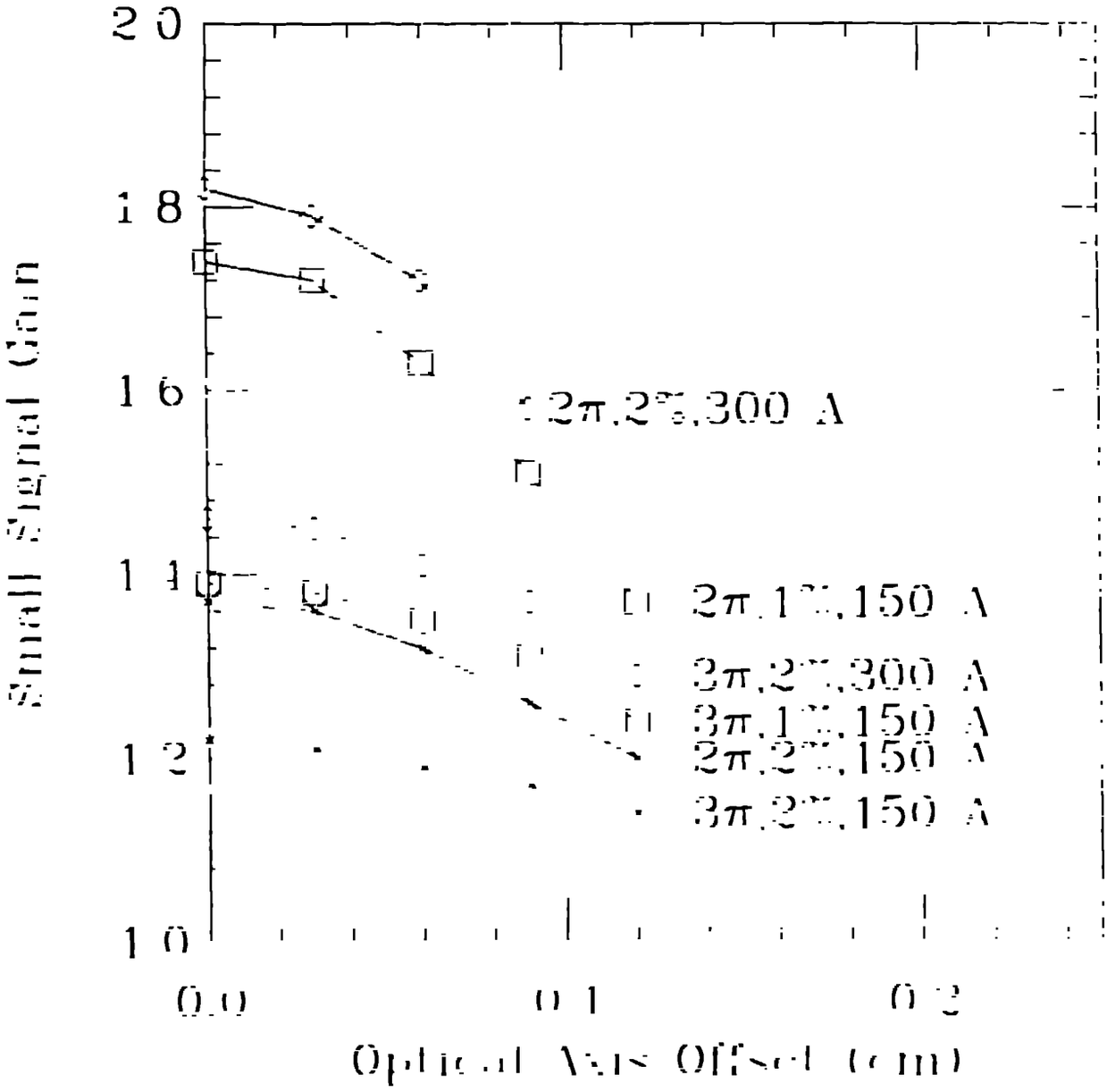
2 0
1 8
1 6
1 4
1 2
1 0
0.0
0 1
0 2
Small Signal Gain
Optical Axis Offset (cm)
2π,2%,300 A
2π,1%,150 A
3π,2%,300 A
3π,1%,150 A
2π,2%,150 A
3π,2%,150 A

FIGURE 1

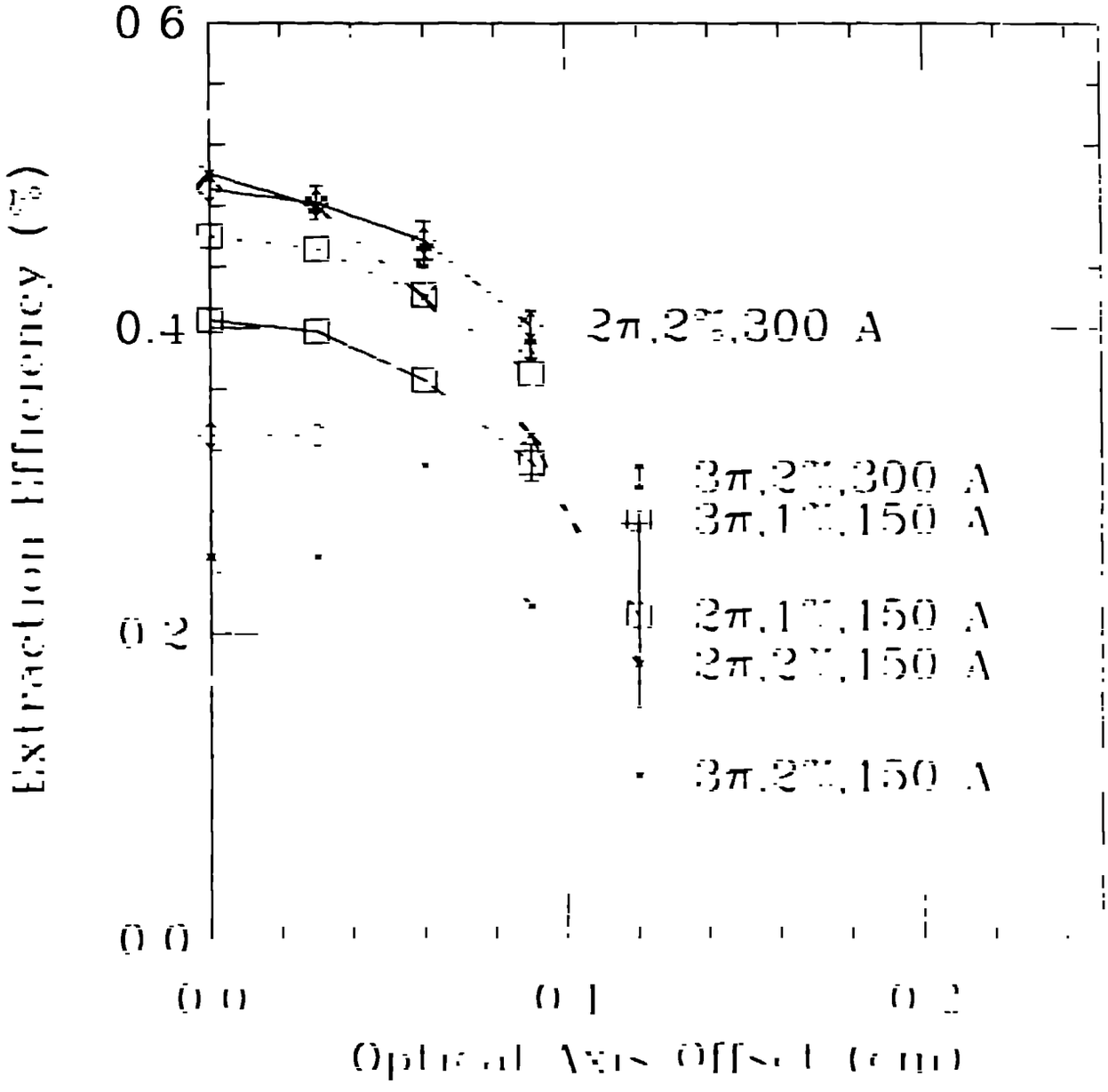
0.6
0.4
0.2
0.0
0.0
0.1
0.2
Extraction Efficiency (%)
Optical Axis Offset (cm)
2π,2%,300 A
3π,2%,300 A
3π,1%,150 A
2π,1%,150 A
2π,2%,150 A
3π,2%,150 A

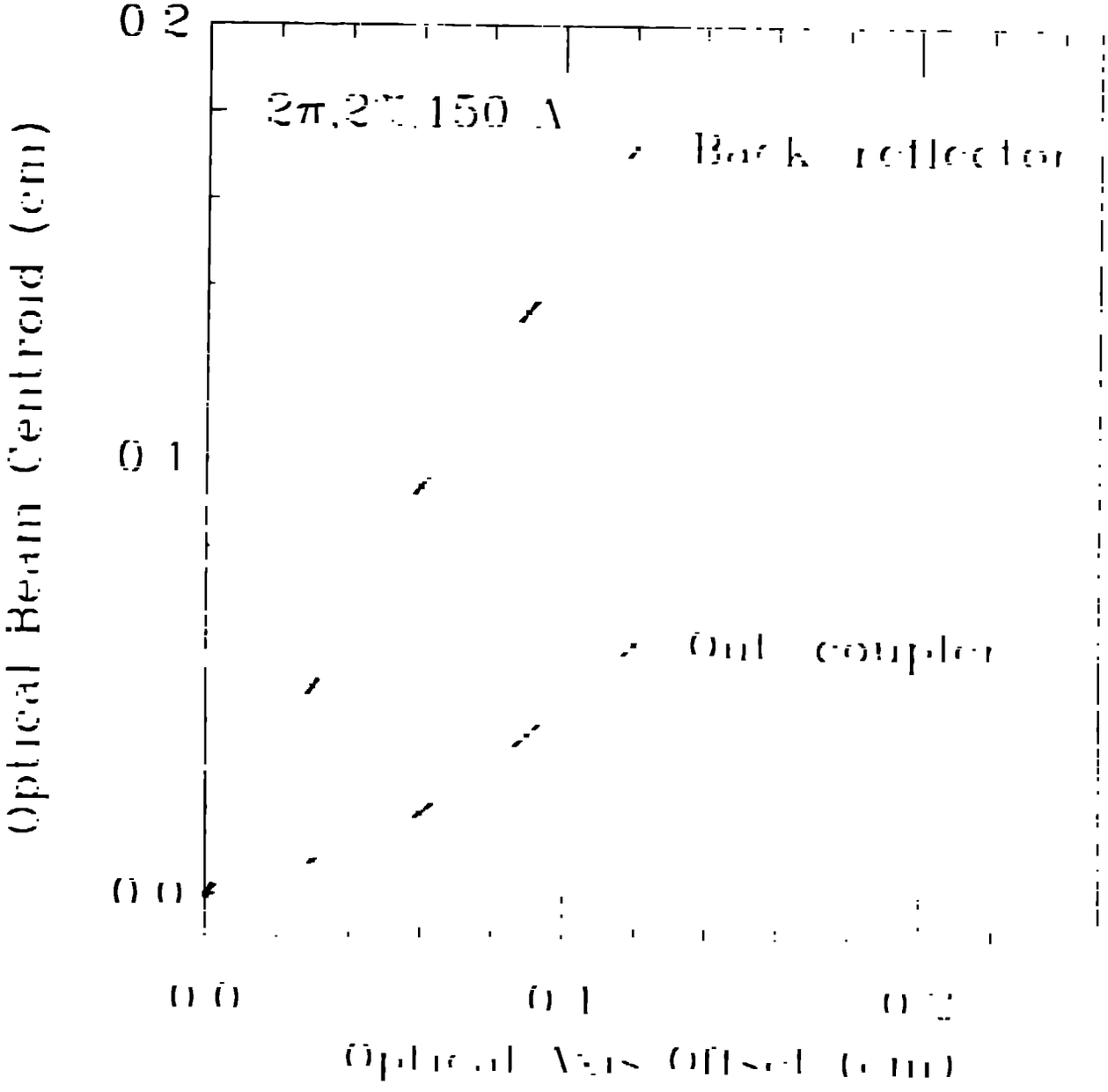

0.2
0.1
0.0
Optical Beam Centroid (cm)
Back reflector
Out coupler
0.0
0.1
0.2
Optical Axis Offset (cm)

FIGURE 6

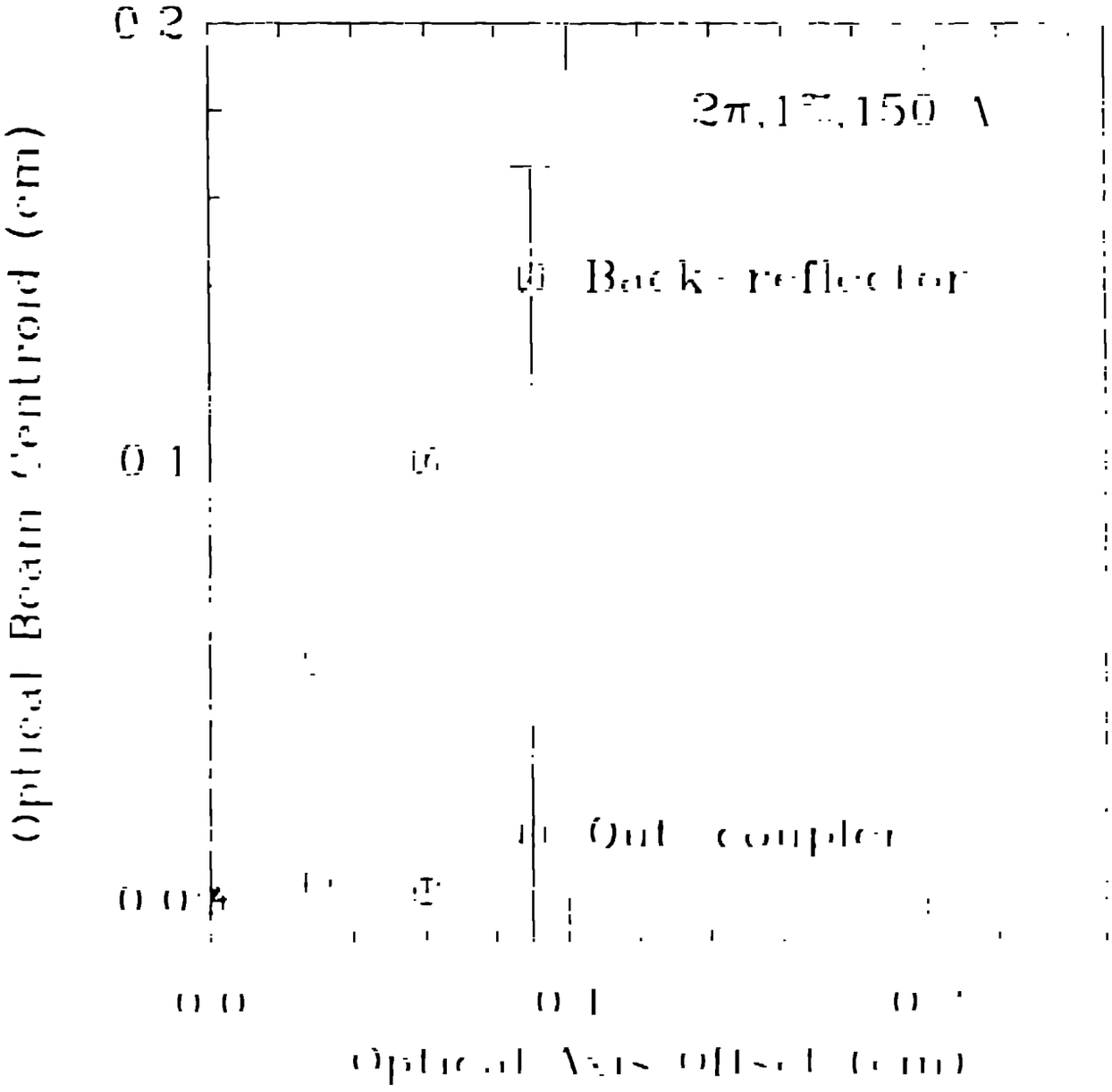
Back reflector
Out coupler
Optical Beam Centroid (cm)
Optical Axis Offset (cm)

Figure 8

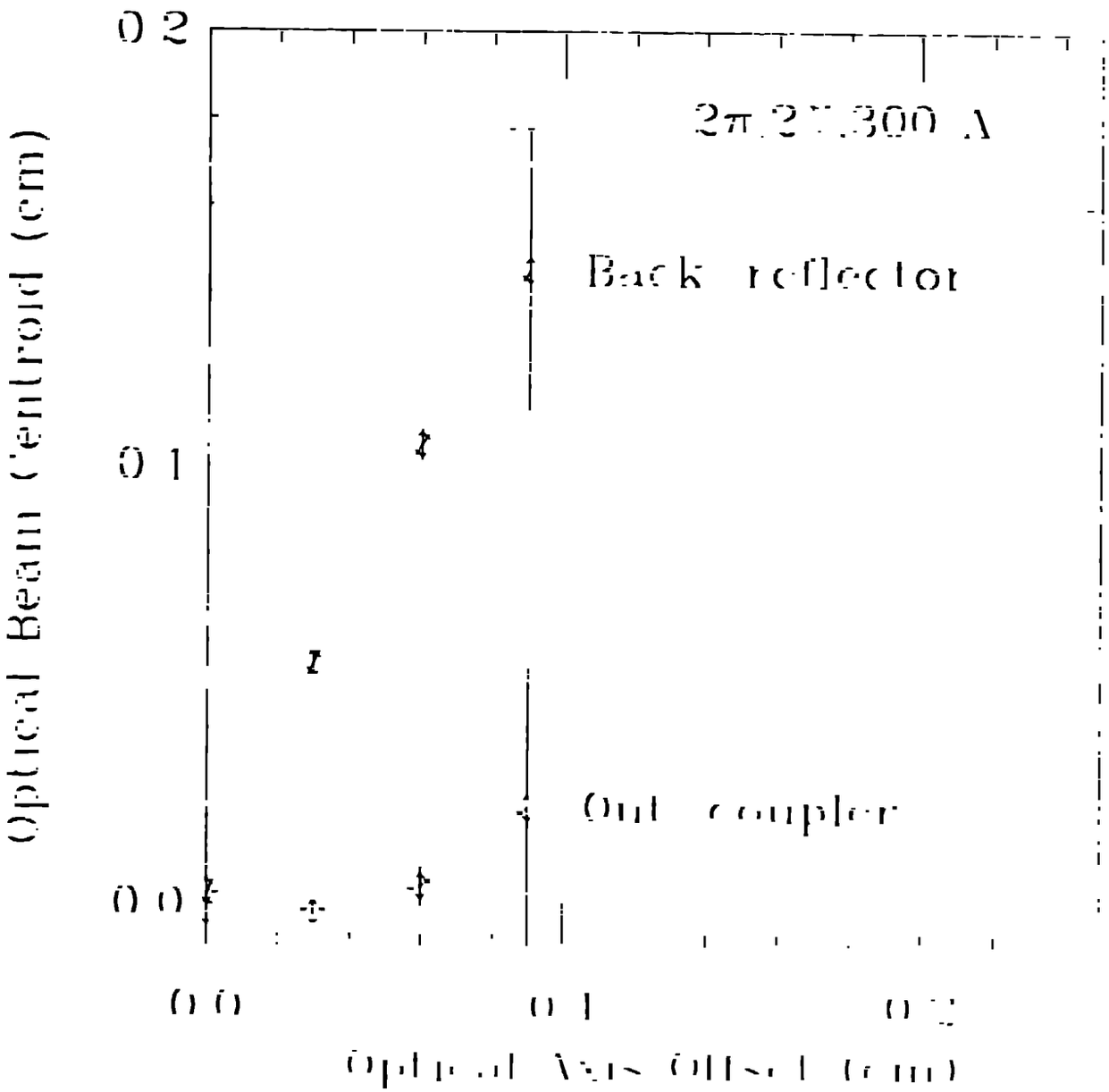

0.2
0.1
0.0
Optical Beam Centroid (cm)
Back reflector
Out coupler
0.0
0.1
0.2
Optical Axis Offset (cm)

FIGURE 6

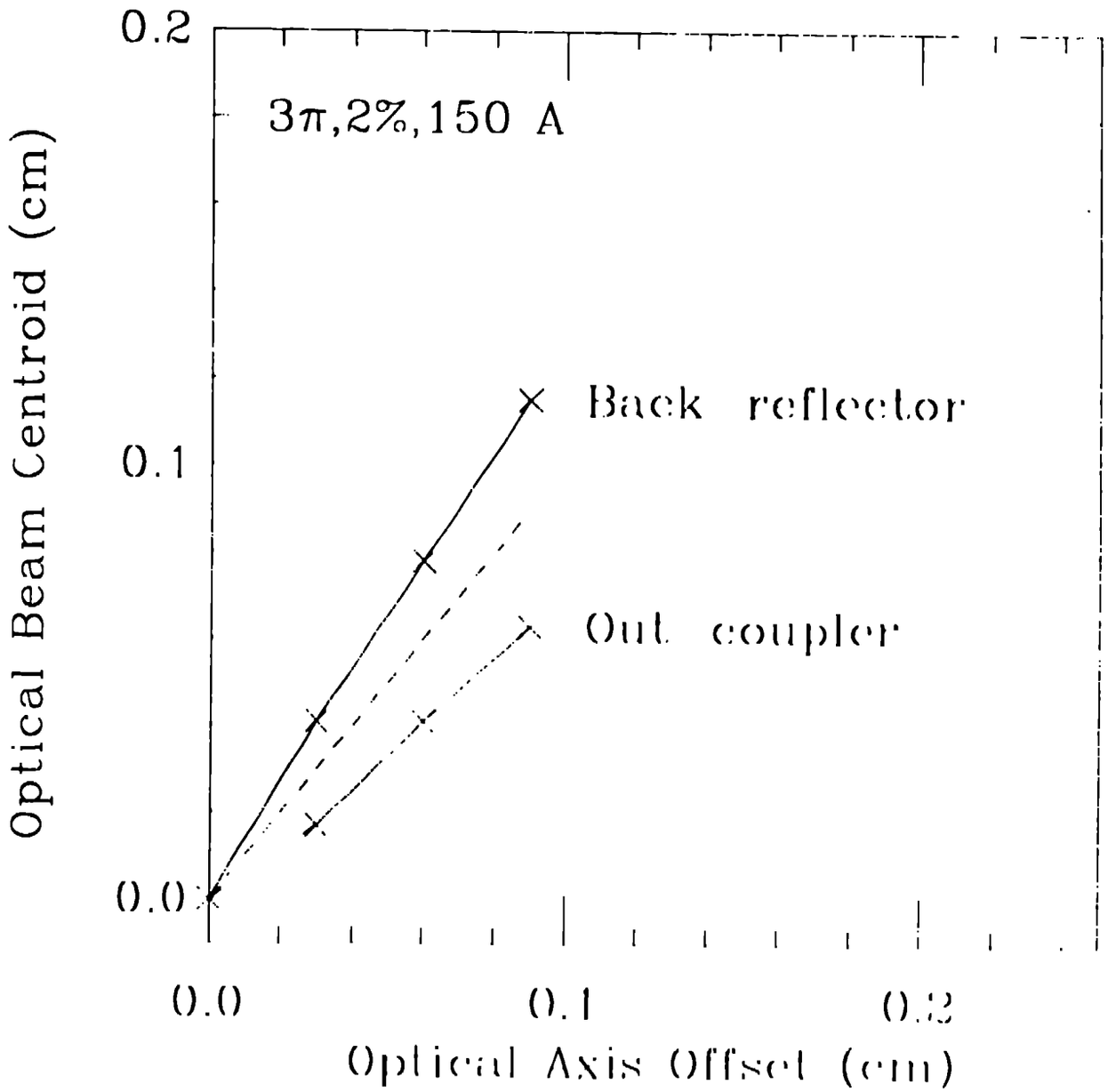
0.2
3π,2%,150 A
Back reflector
0.1
Out coupler
0.0
0.0
0.1
0.2
Optical Beam Centroid (cm)
Optical Axis Offset (cm)

FIGURE 3D

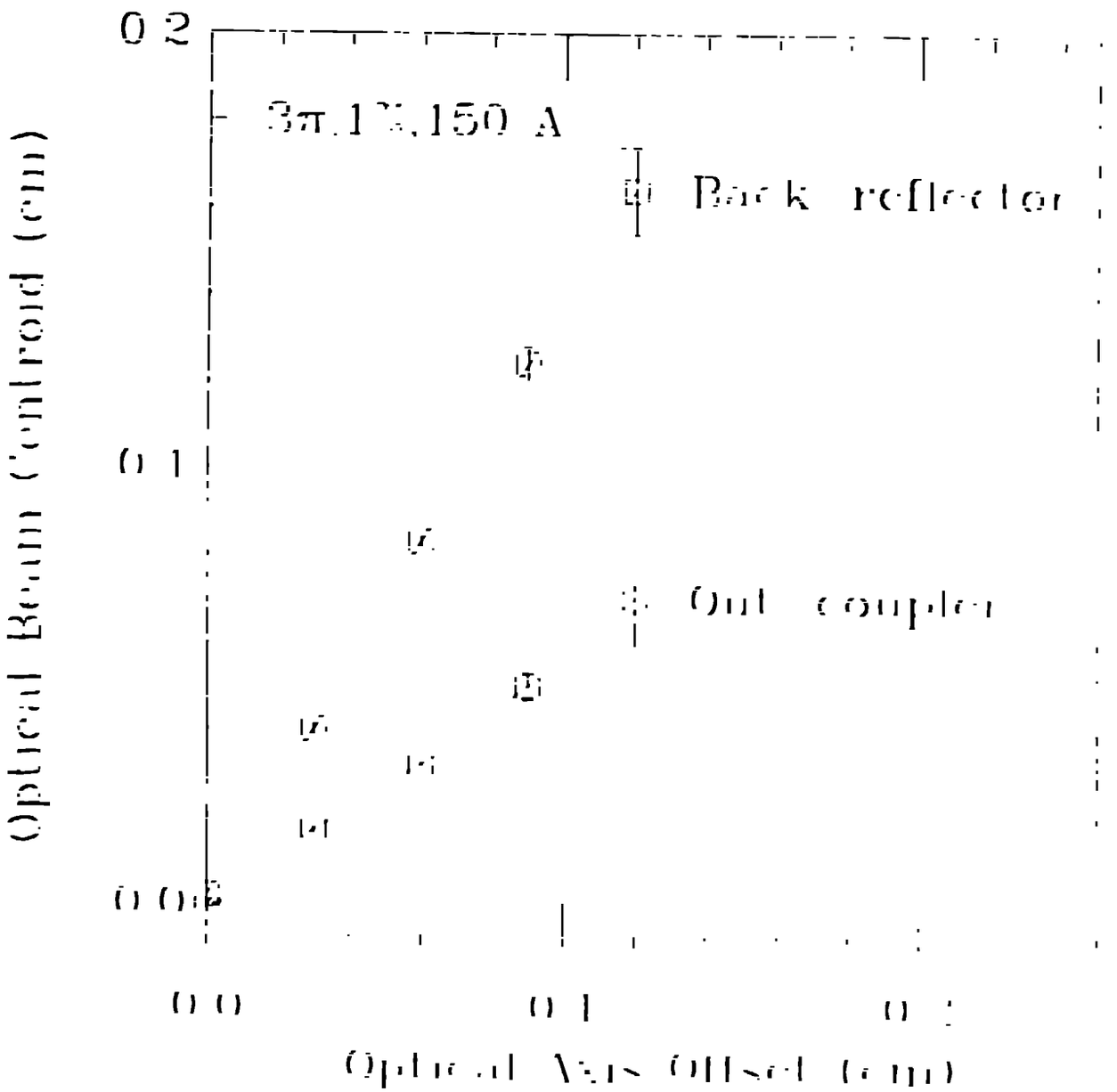
0.2
0.1
0.0
0.0
0.1
0.2
Optical Beam Centroid (cm)
Optical Axis Offset (cm)
3π,17%,150 A
Back reflector
Out coupler

Figure 8

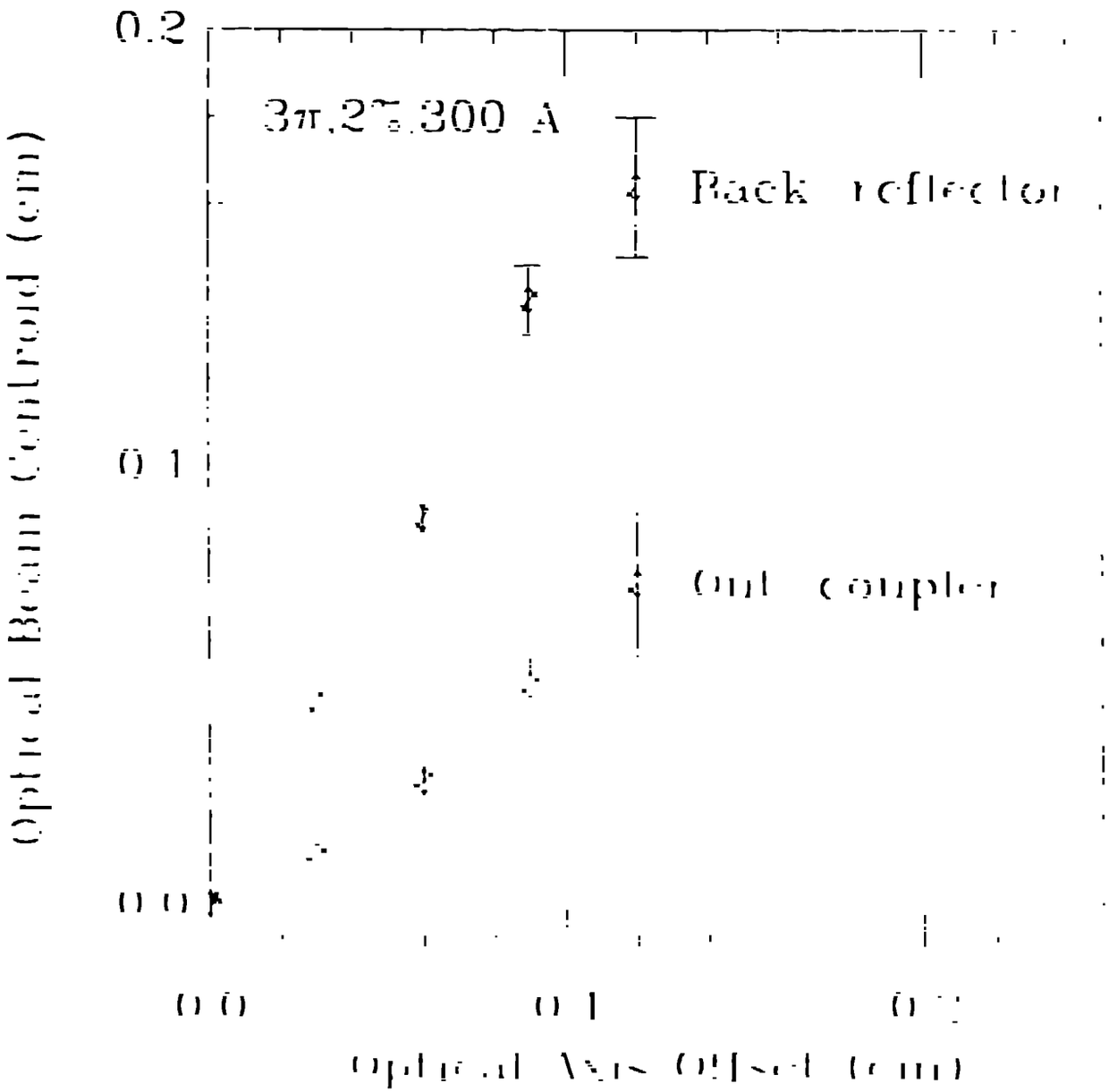
0.2
0.1
0.0
3π,2π,300 A
Back reflector
Out coupler
0.0
0.1
0.2
Optical Axis Offset (cm)
Optical Beam Centroid (cm)

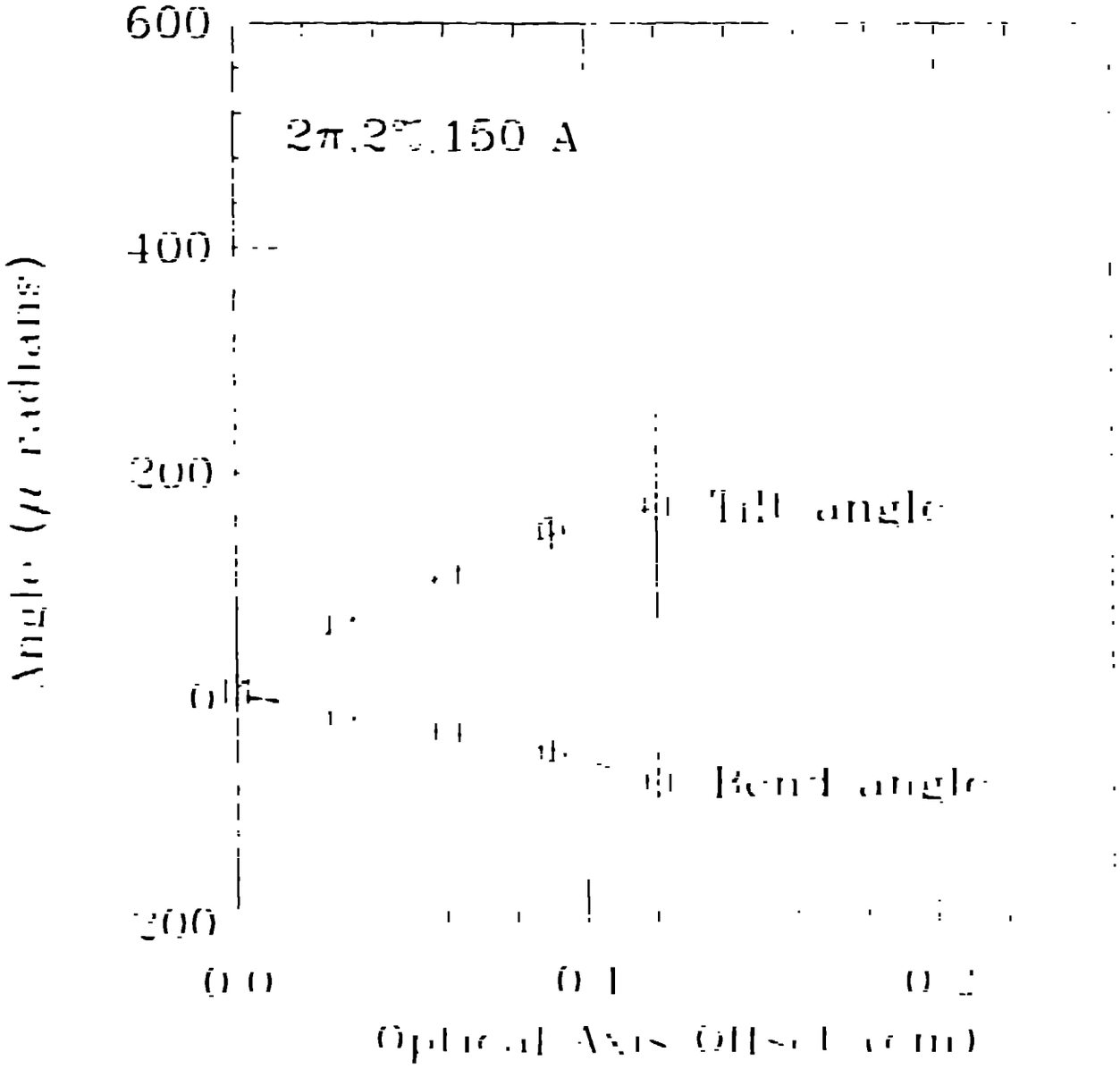
600
400
200
0
-200
2π.2%.150 A
Tilt angle
Bend angle
Angle (μ radians)
0.0
0.1
0.2
Optical Axis Offset (cm)

Figure 5

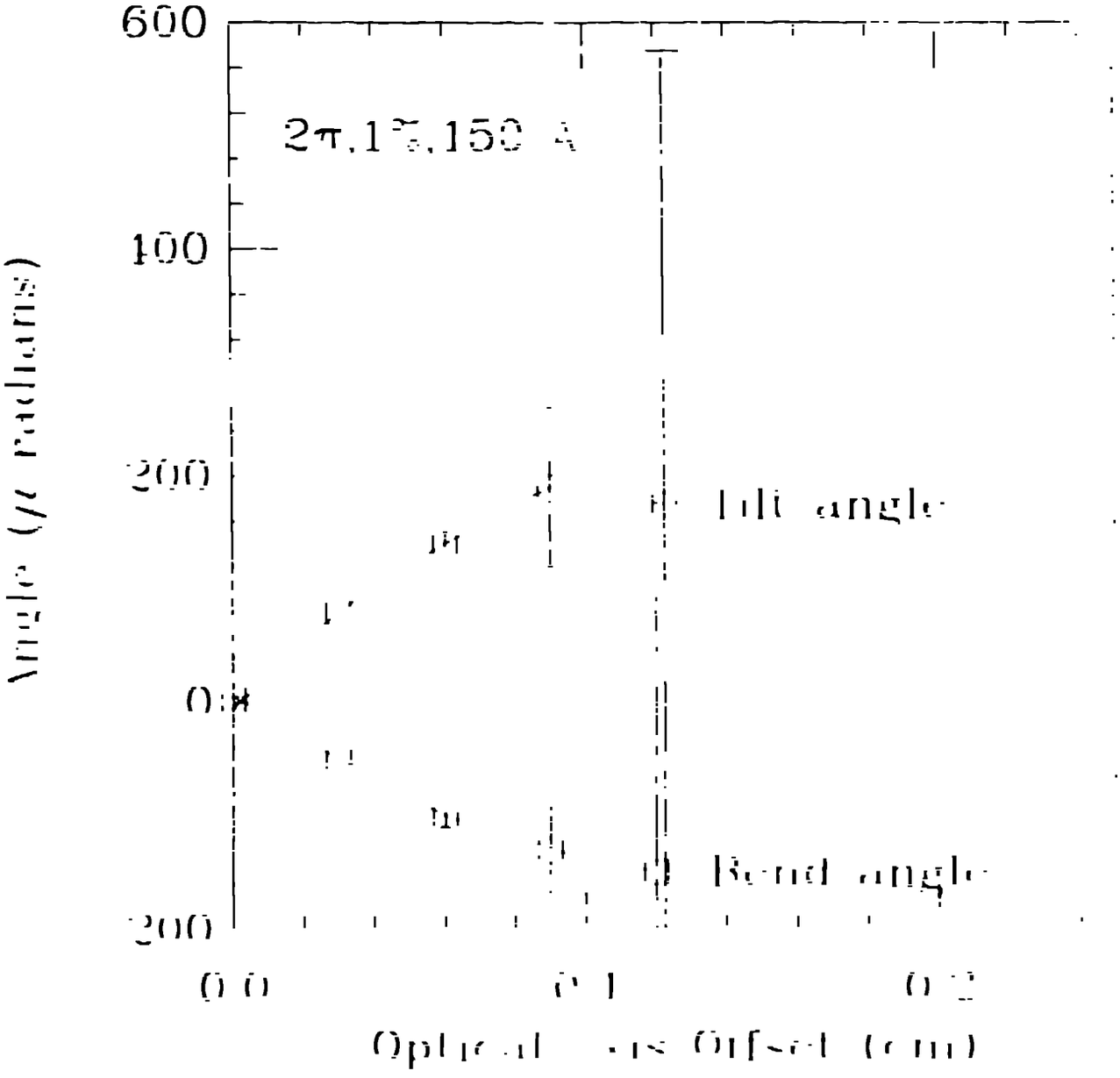

600
400
200
0
-200
2π,1%,150 A
Tilt angle
Bend angle
0.0
0.1
0.2
Angle (μ radians)
Optical axis Offset (cm)

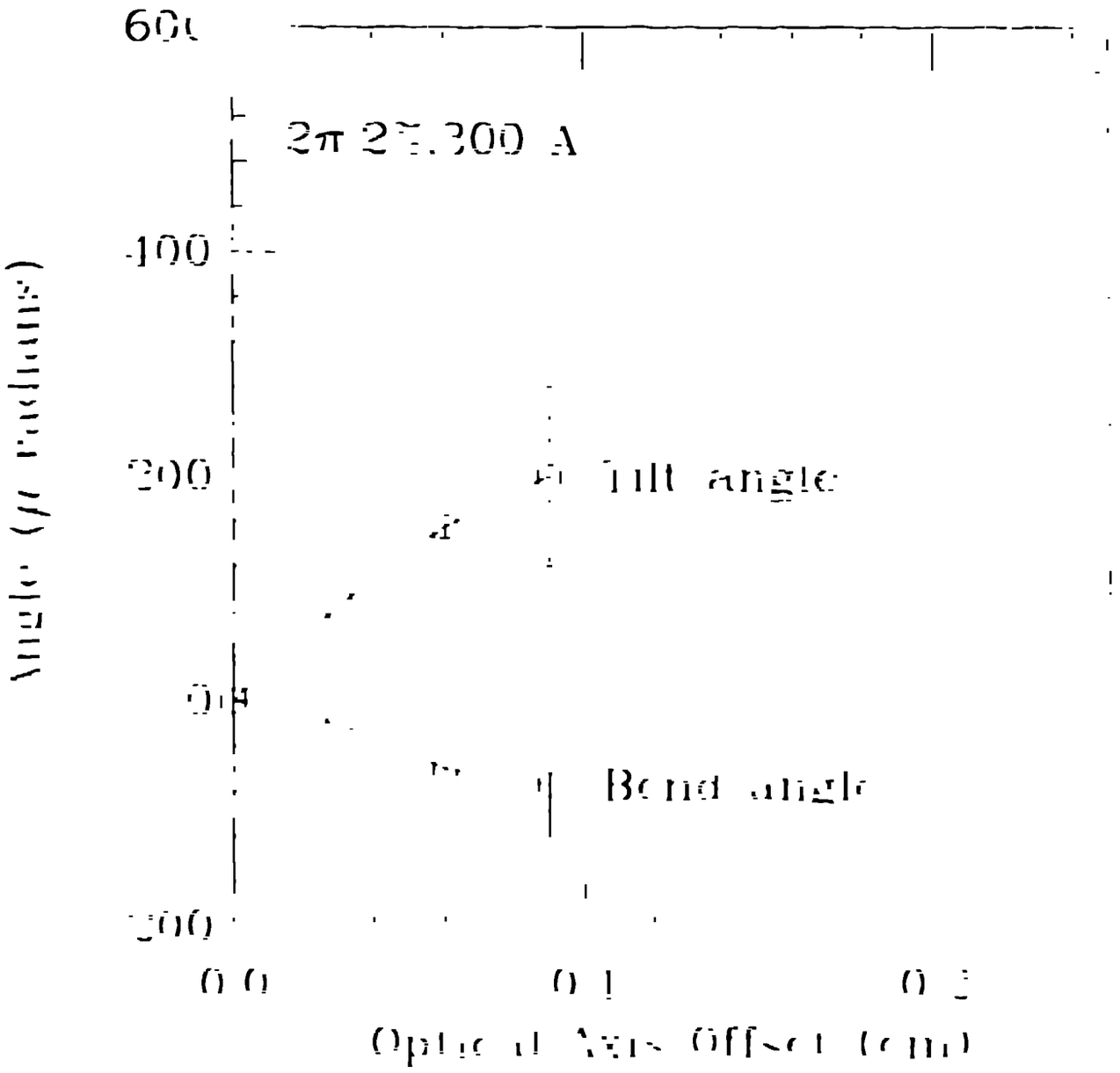
2π 27.300 A
Tilt angle
Bend angle
Angle (μ radians)
Optical Axis Offset (cm)

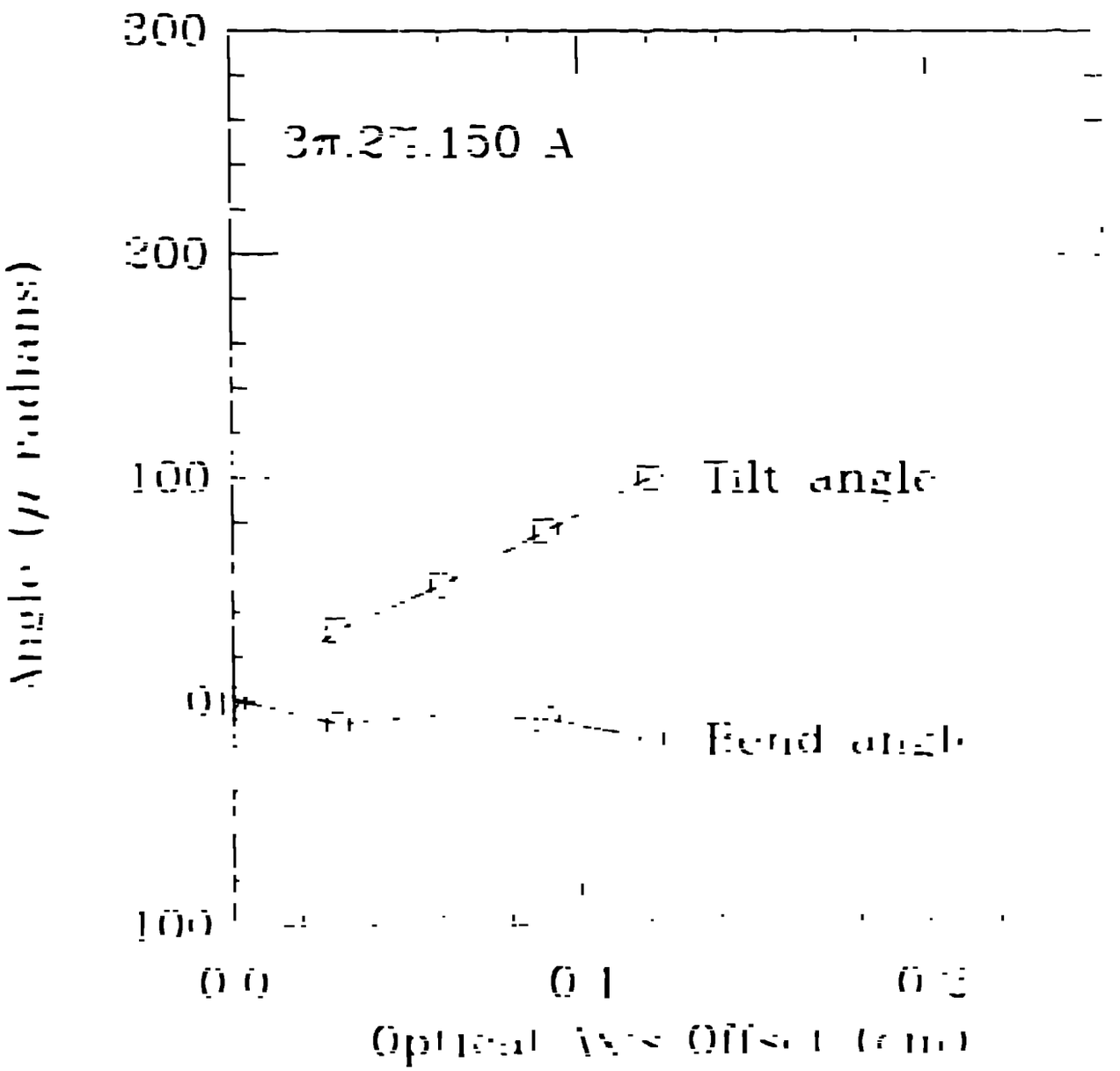
300
200
100
0
100
3π.2π.150 A
Tilt angle
Bend angle
Angle (μ radians)
0.0
0.1
0.3

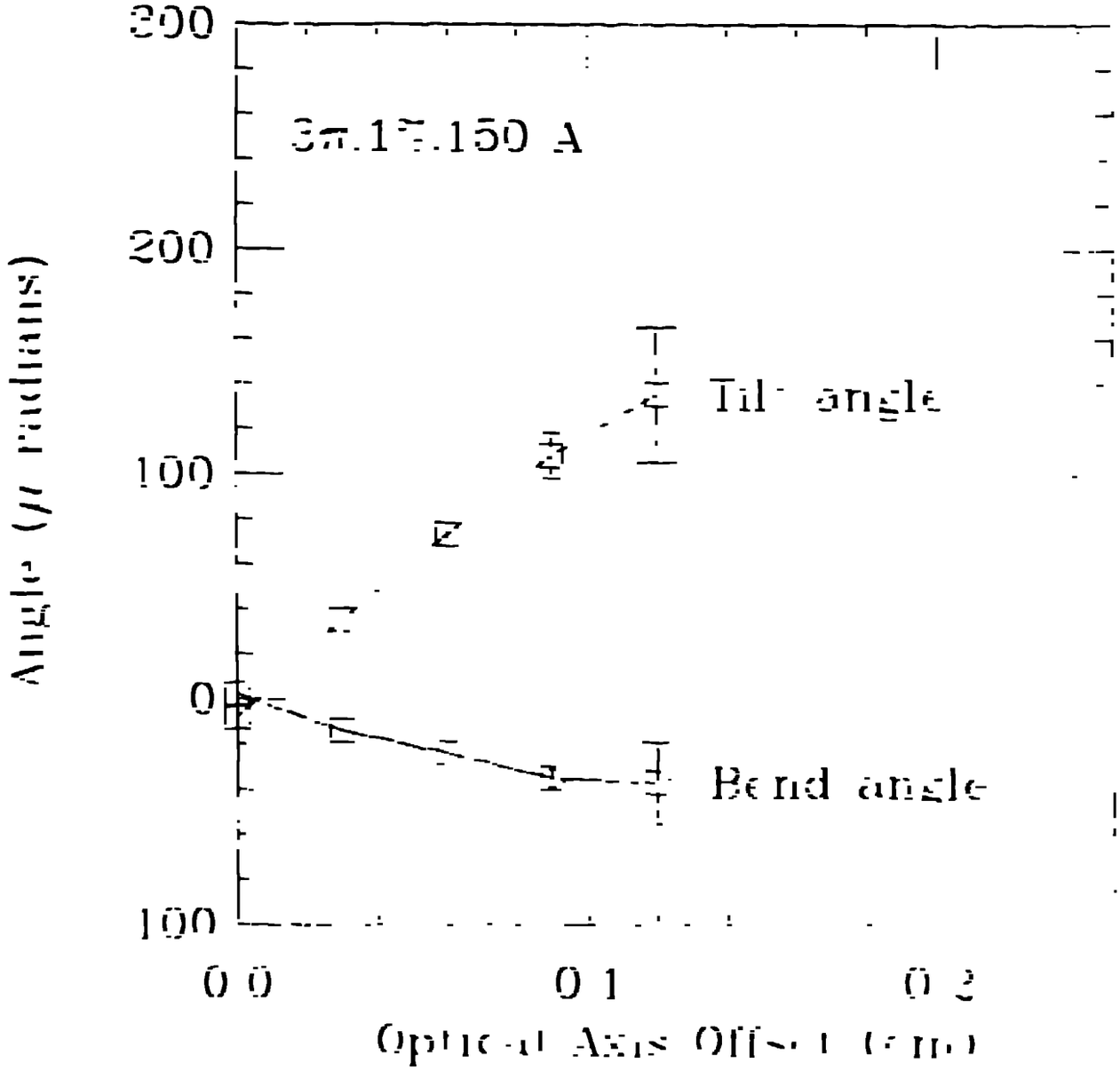
3π.1?.150 A
Tilt angle
Bend angle
Angle (μ radians)
Optical Axis Offset (cm)
300
200
100
0
100
0.0
0.1
0.2

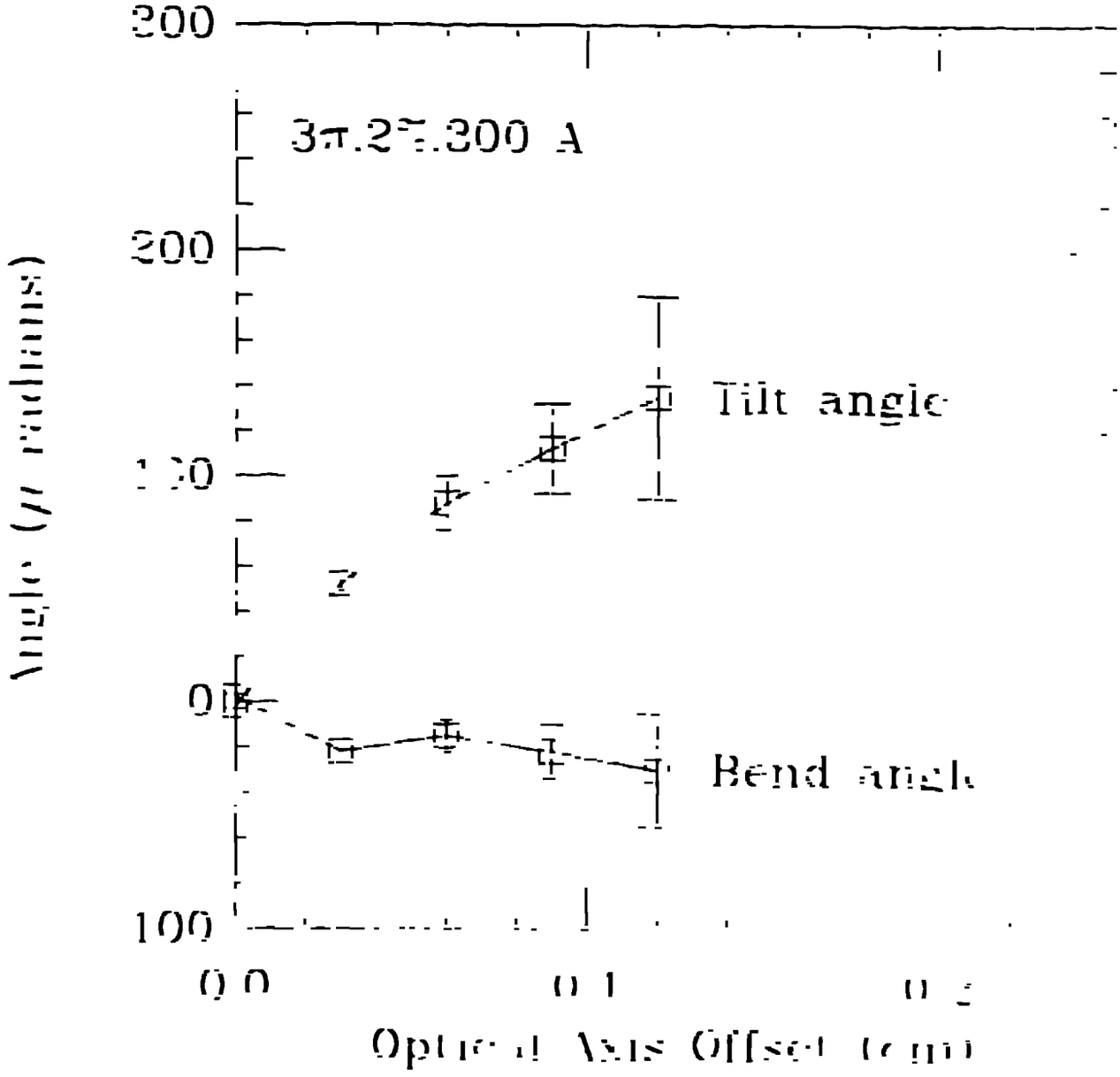

300
200
100
0
100
3π.2%.300 A
Tilt angle
Bend angle
Angle (μ radians)
0.0
0.1
Optical Axis Offset (cm)

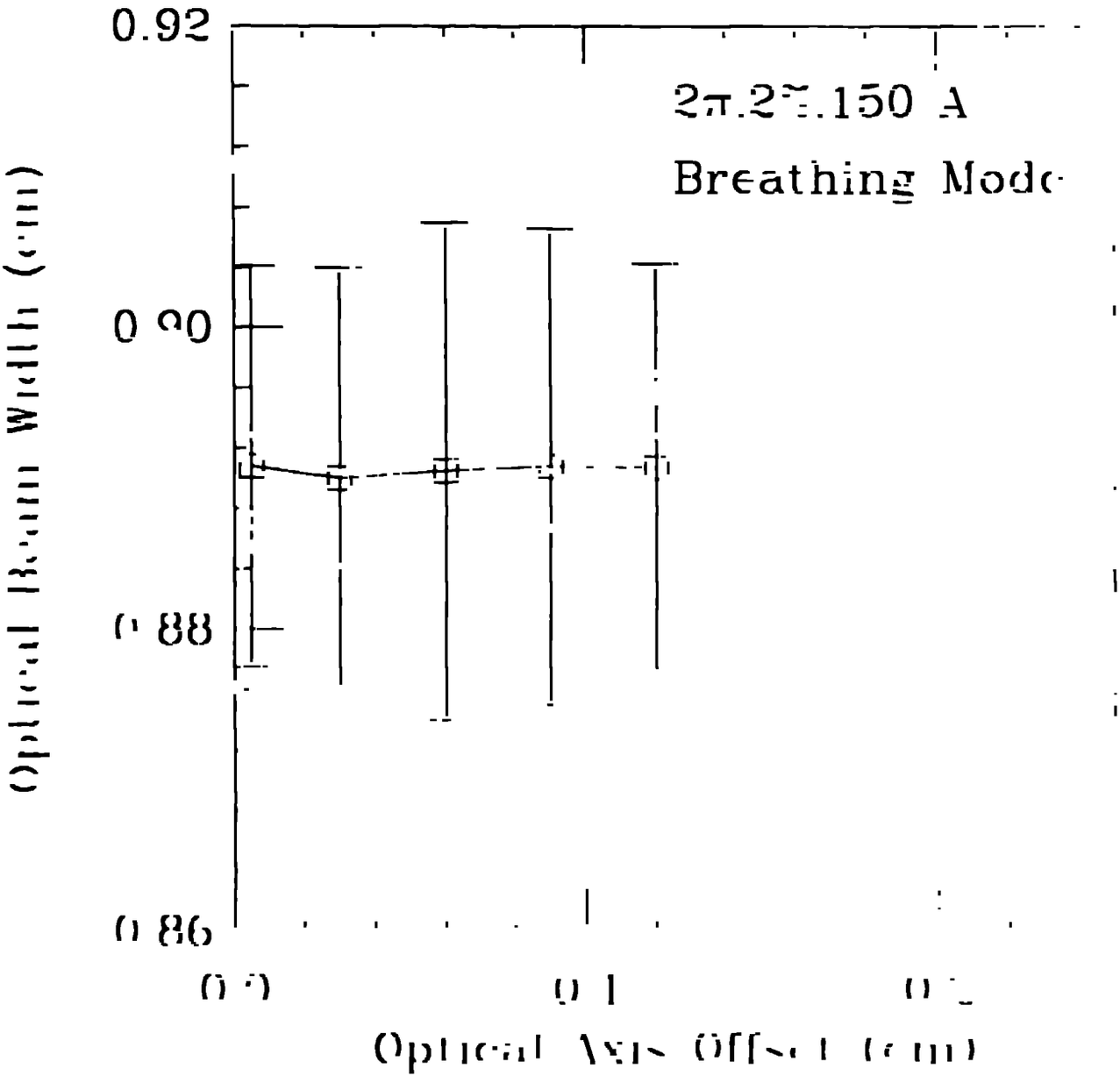
0.92
0.90
0.88
0.86
Breathing Mode
Optical Axis Offset (cm)

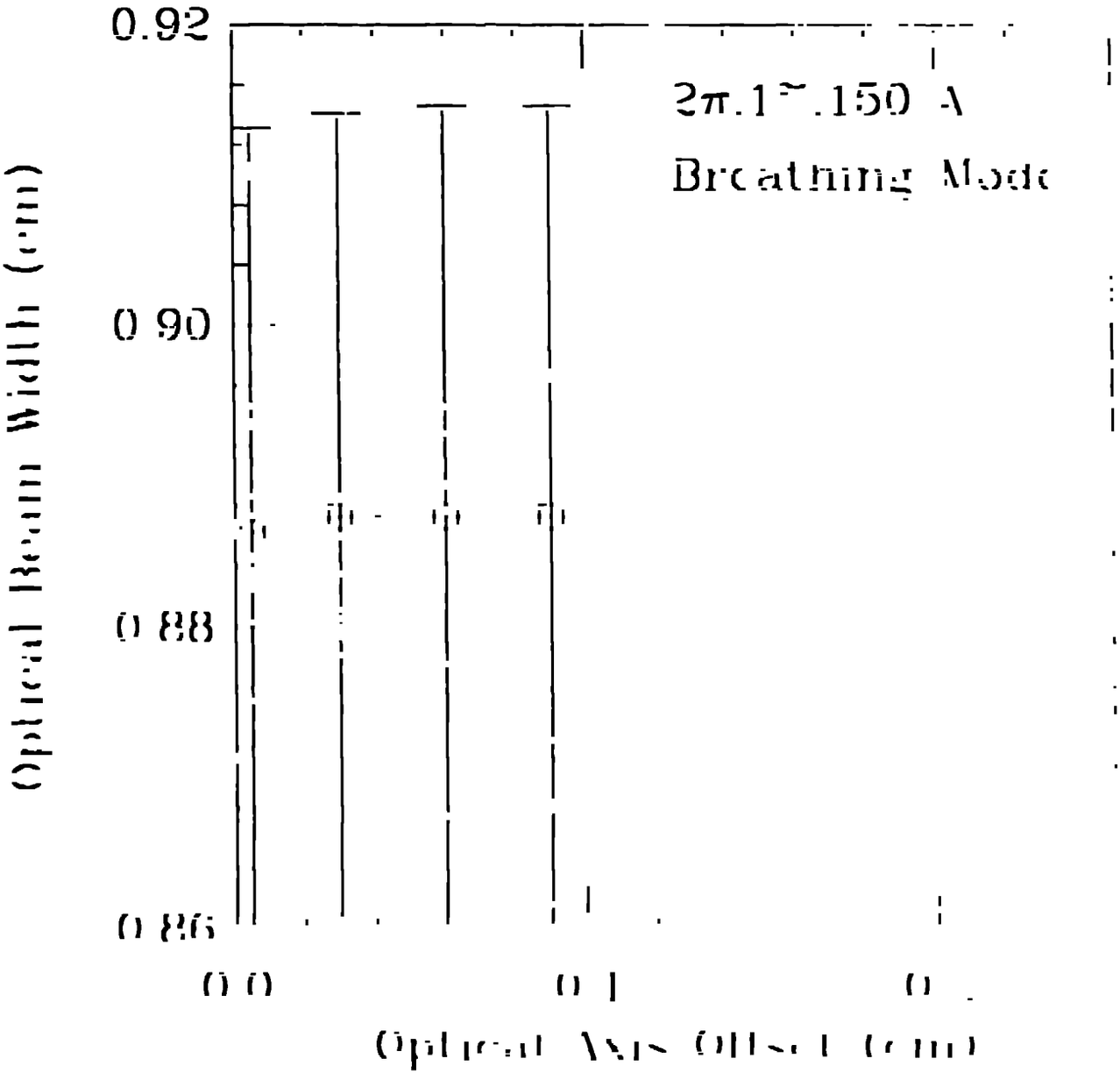
0.92
0.90
0.88
0.86
Optical Beam Width (cm)
2π.1~.150 A
Breathing Mode

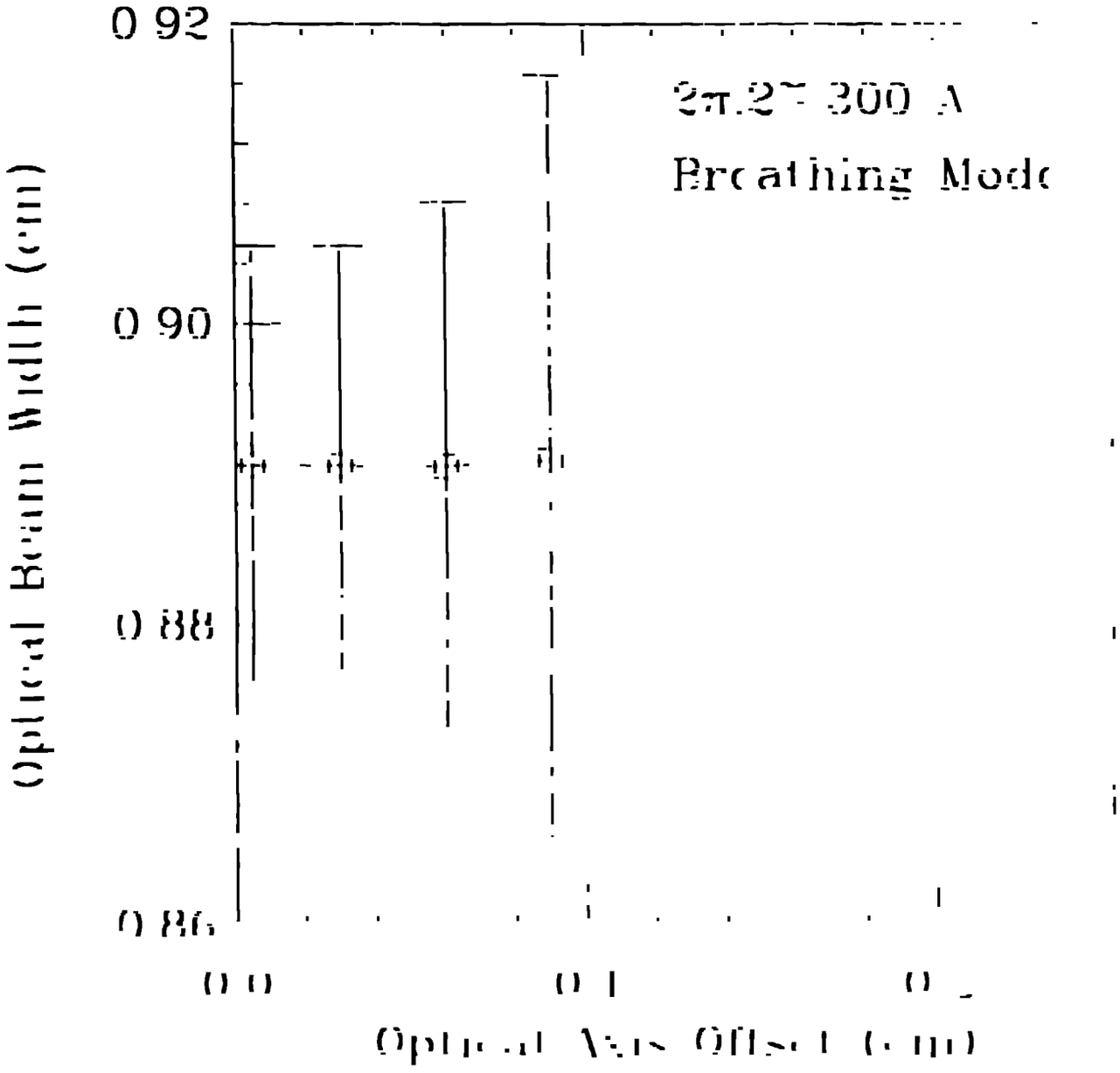
0.92
0.90
0.88
0.86
Optical Beam Width (cm)
Breathing Mode
0.0
0.1

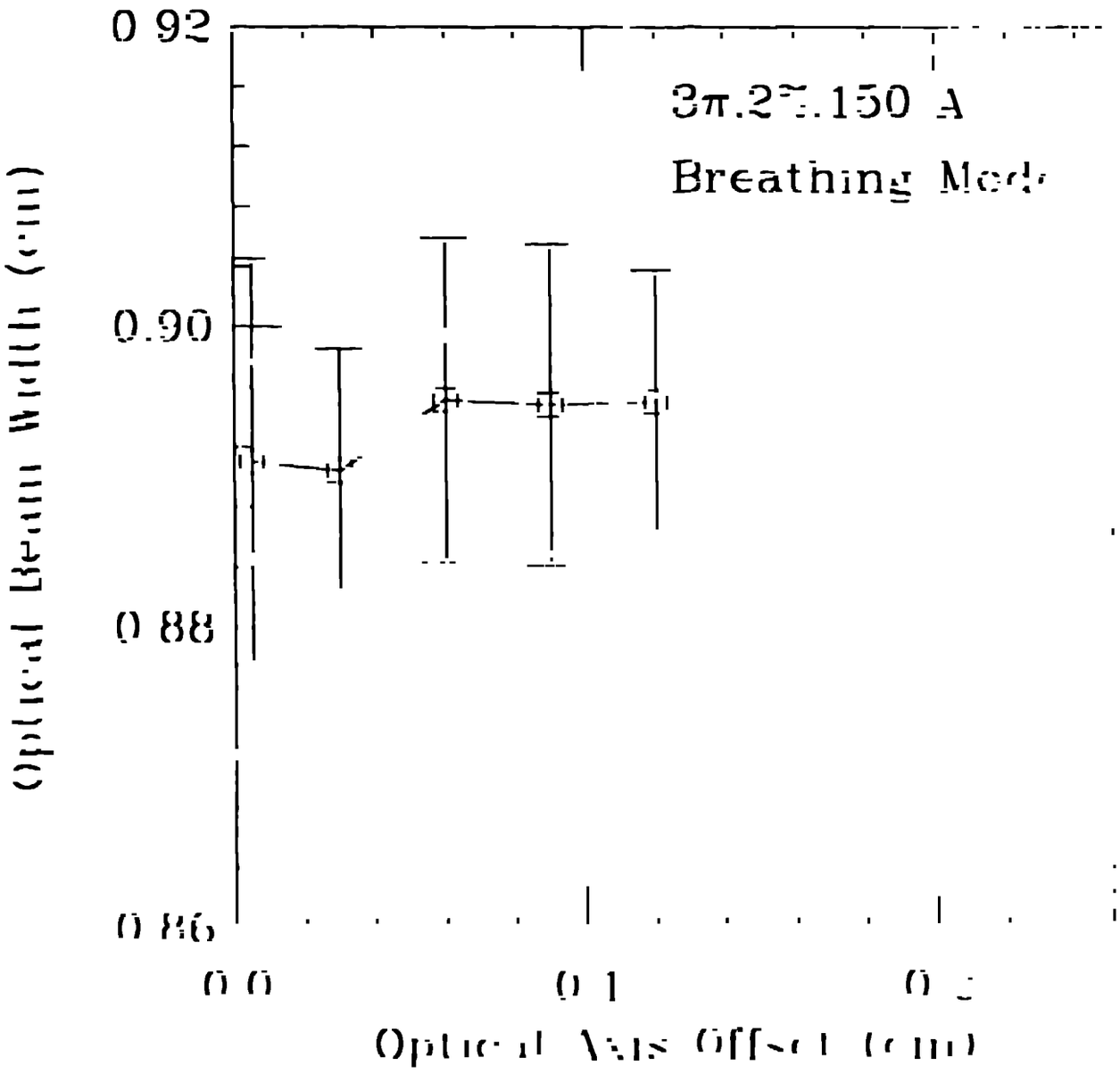
0.92
0.90
0.88
0.86
0.0
0.1
Breathing Mode

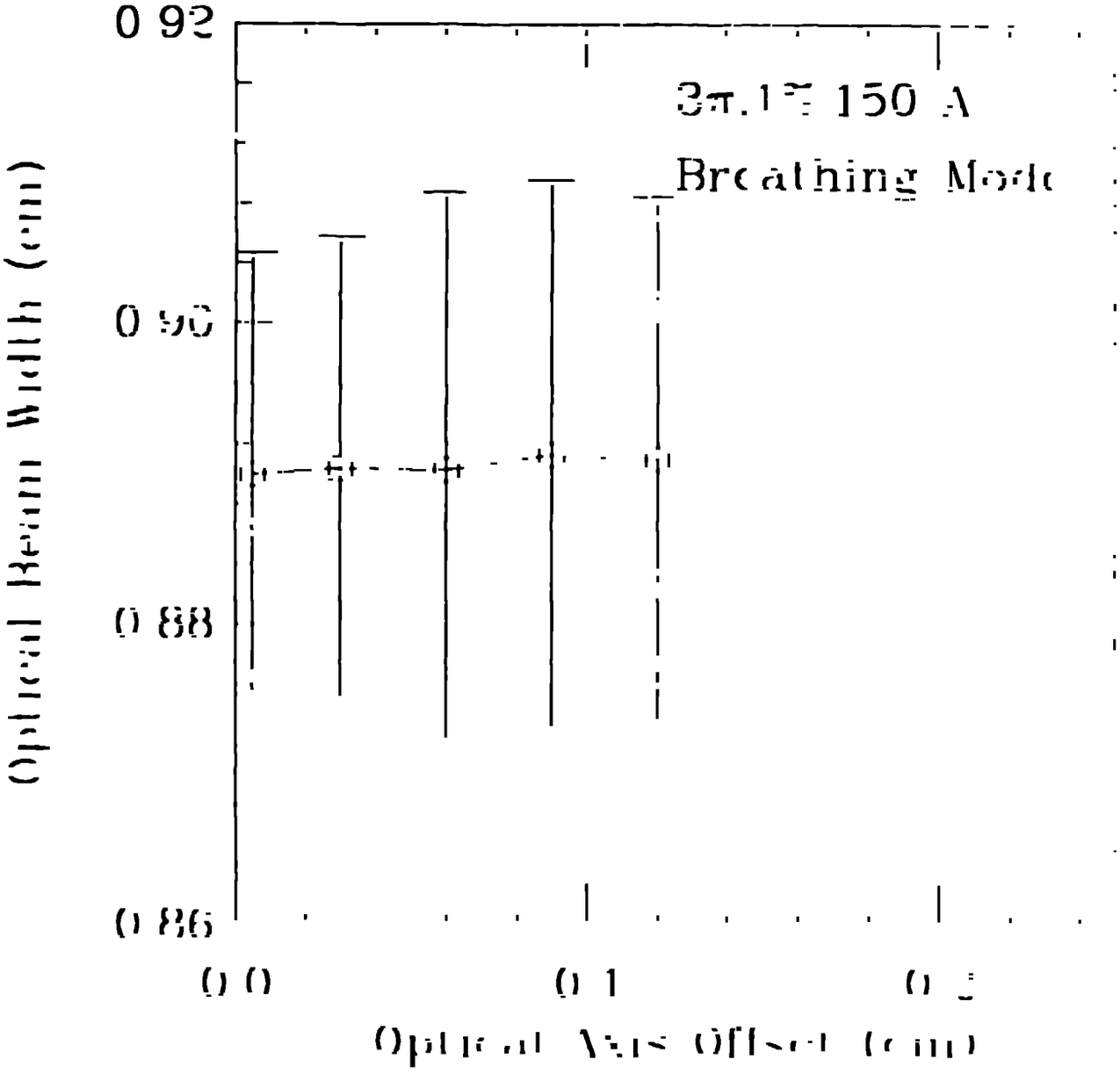

0.92
0.90
0.88
0.86
0.0
0.1
Optical Beam Width (cm)
Breathing Mode

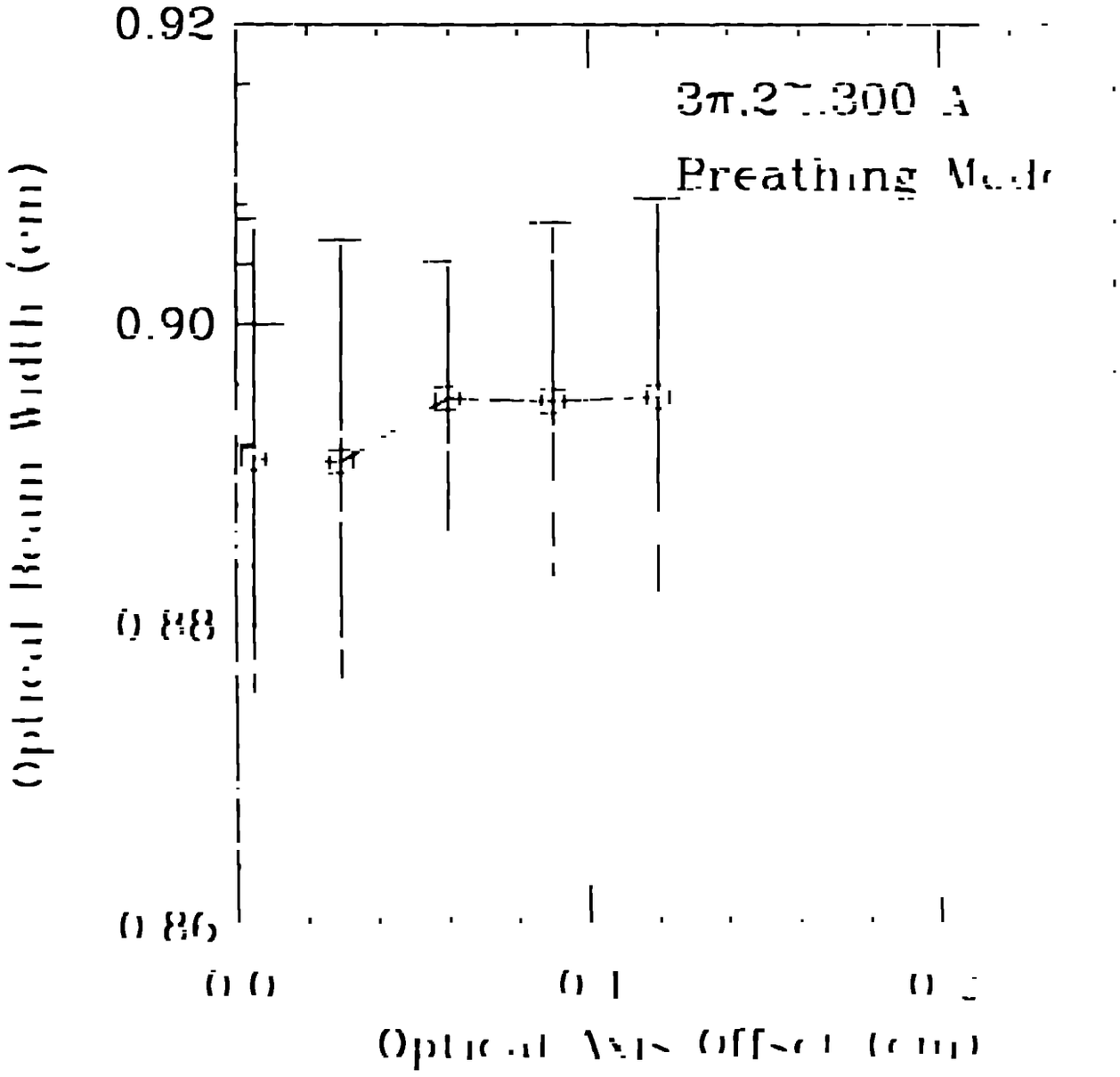
0.92
0.90
3π.2~.300 A
Breathing Mode

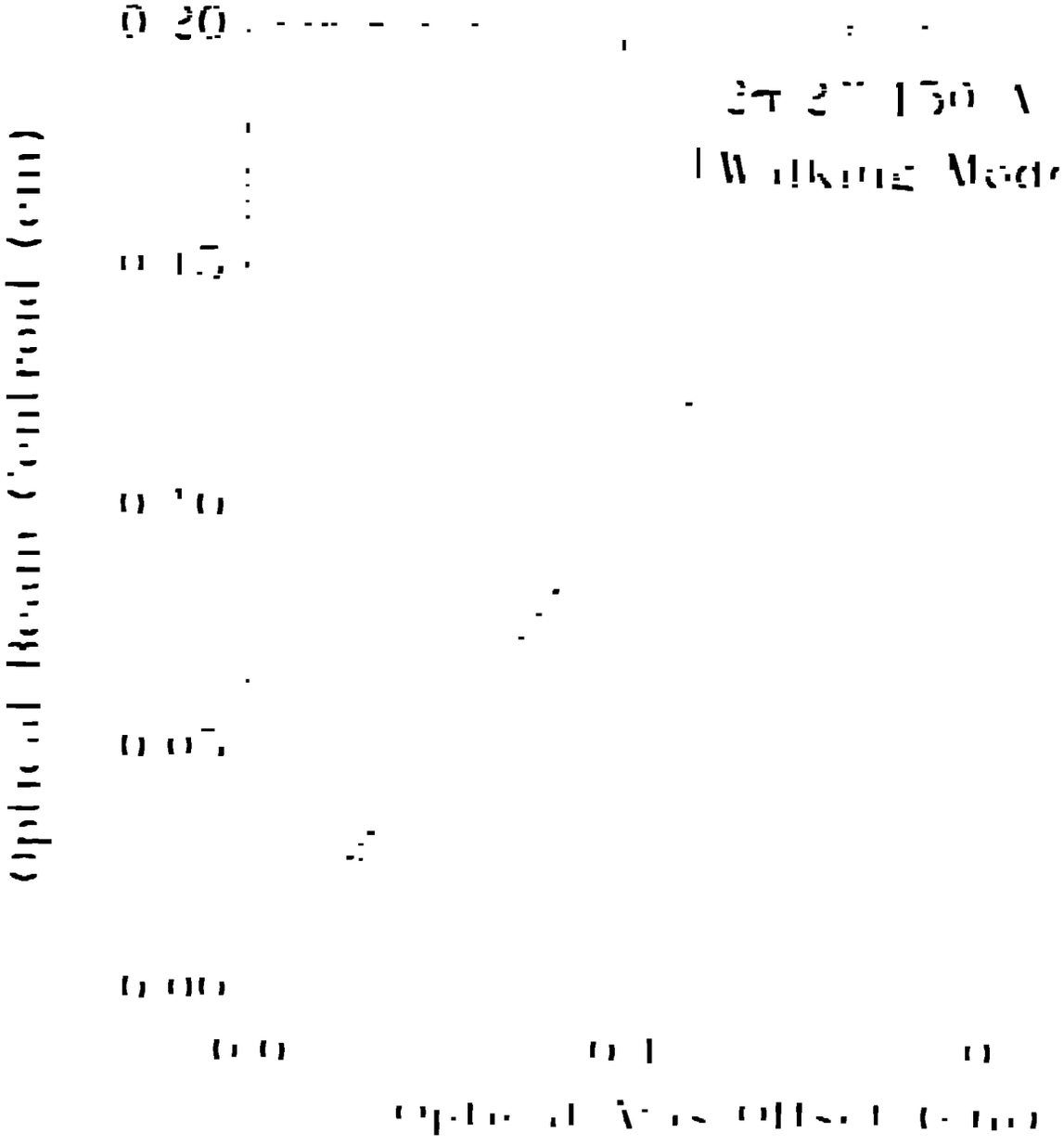

0.20
0.15
0.10
0.05
0.00
0.0
0.1
0
Optical Beam Centroid (cm)
Optical Axis Offset (cm)
Walking Mode

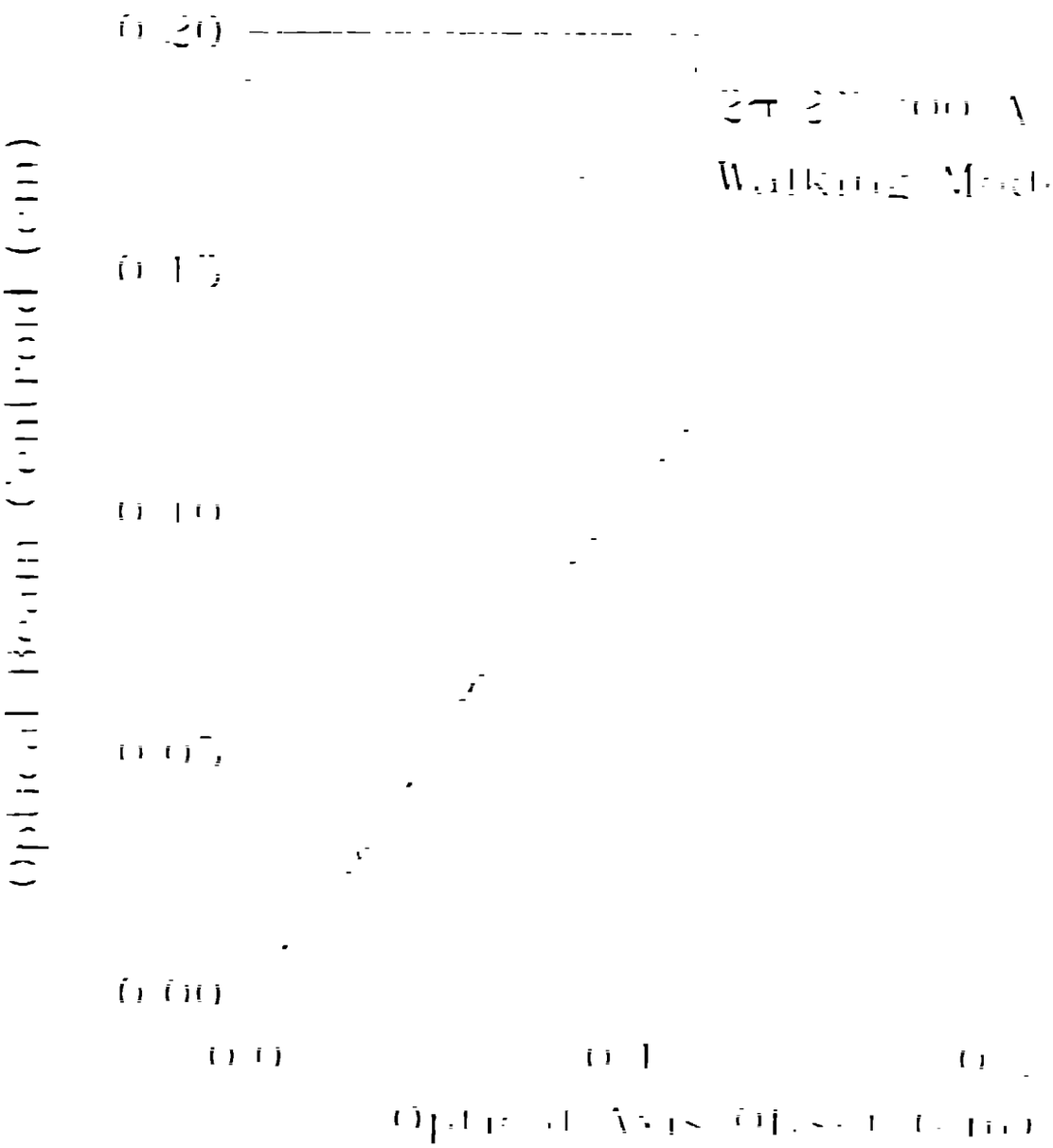
Optical Beam Centroid (cm)
Optical Axis Offset (cm)
Walking Mode

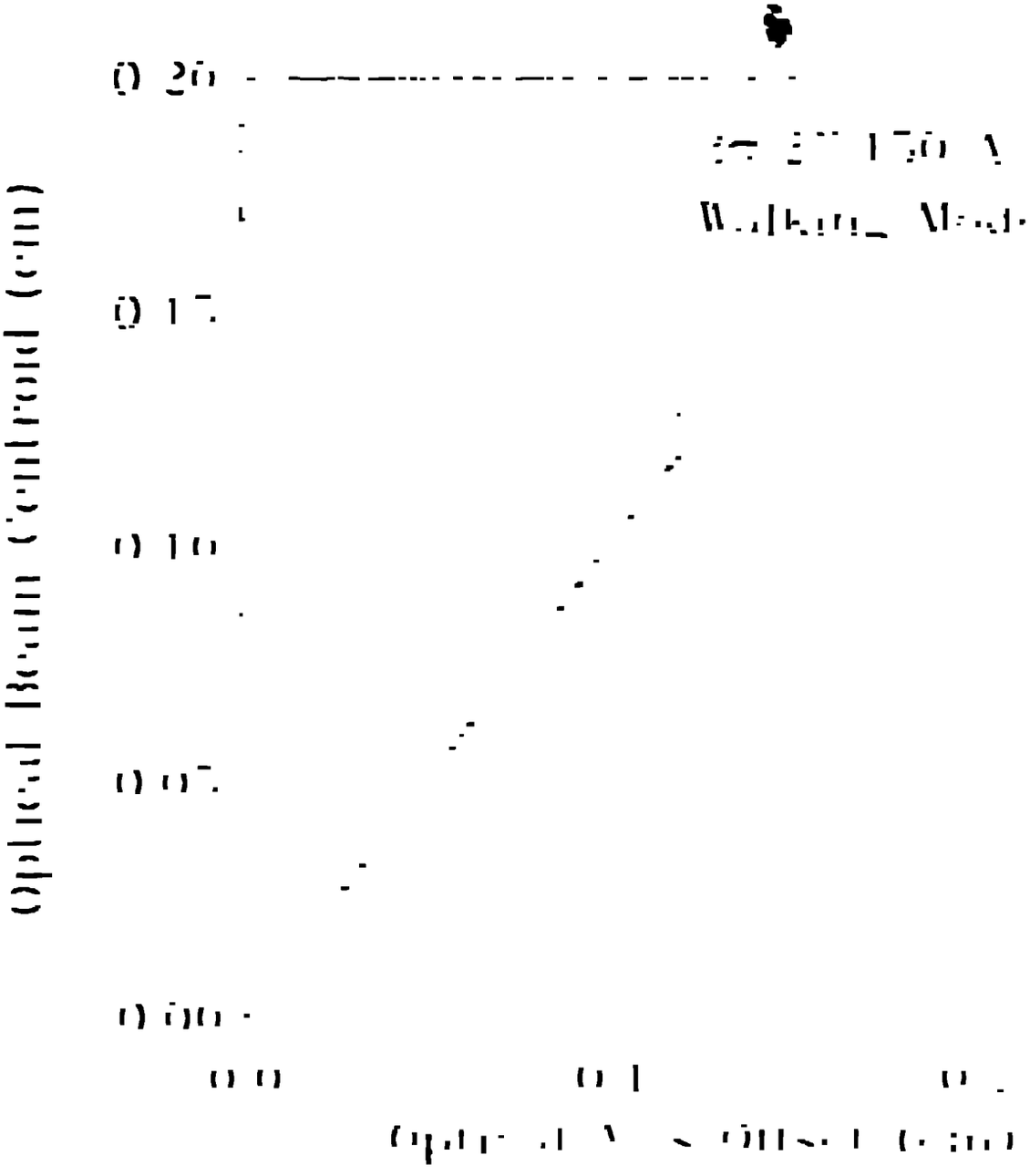

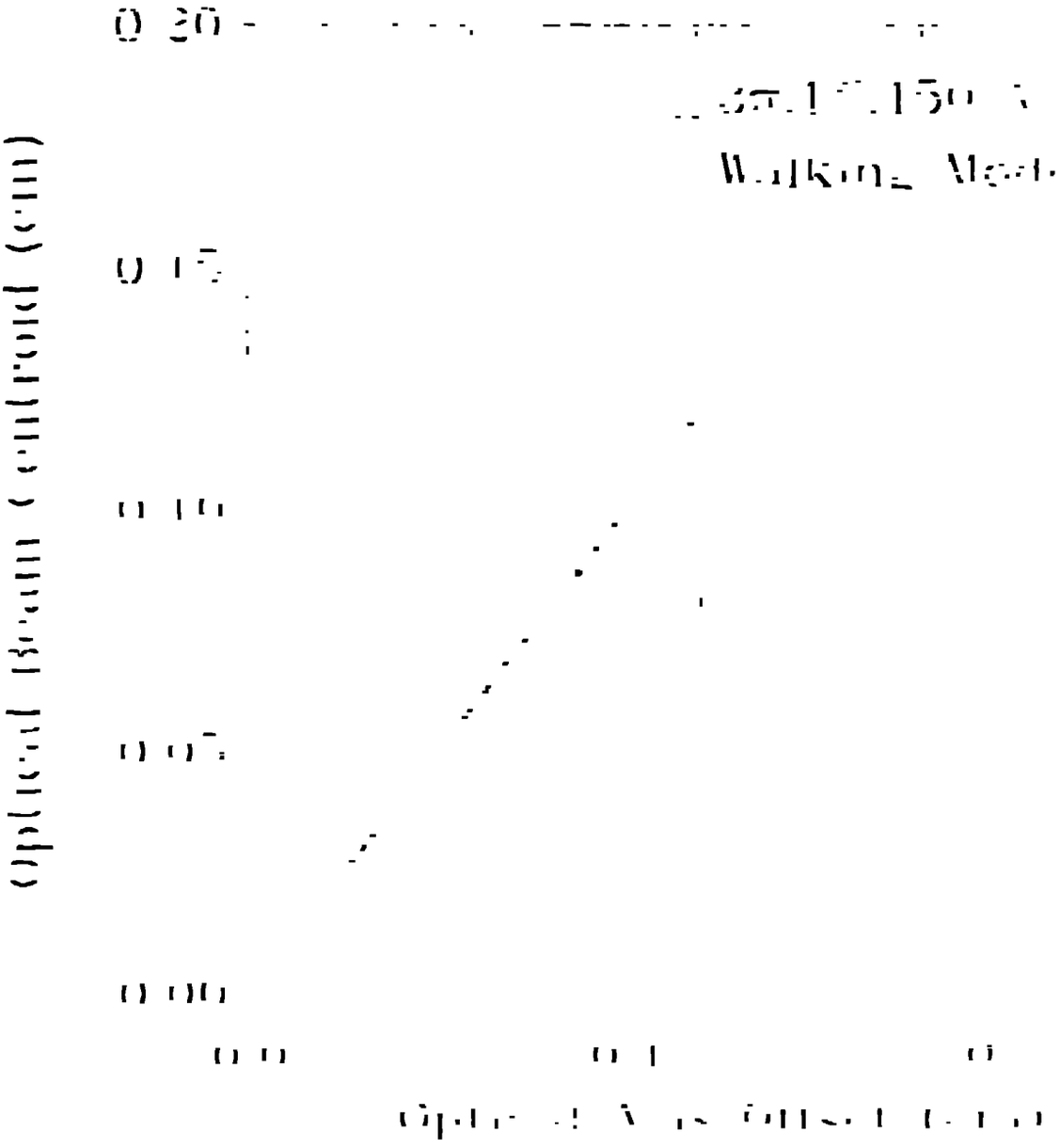
Working Mode

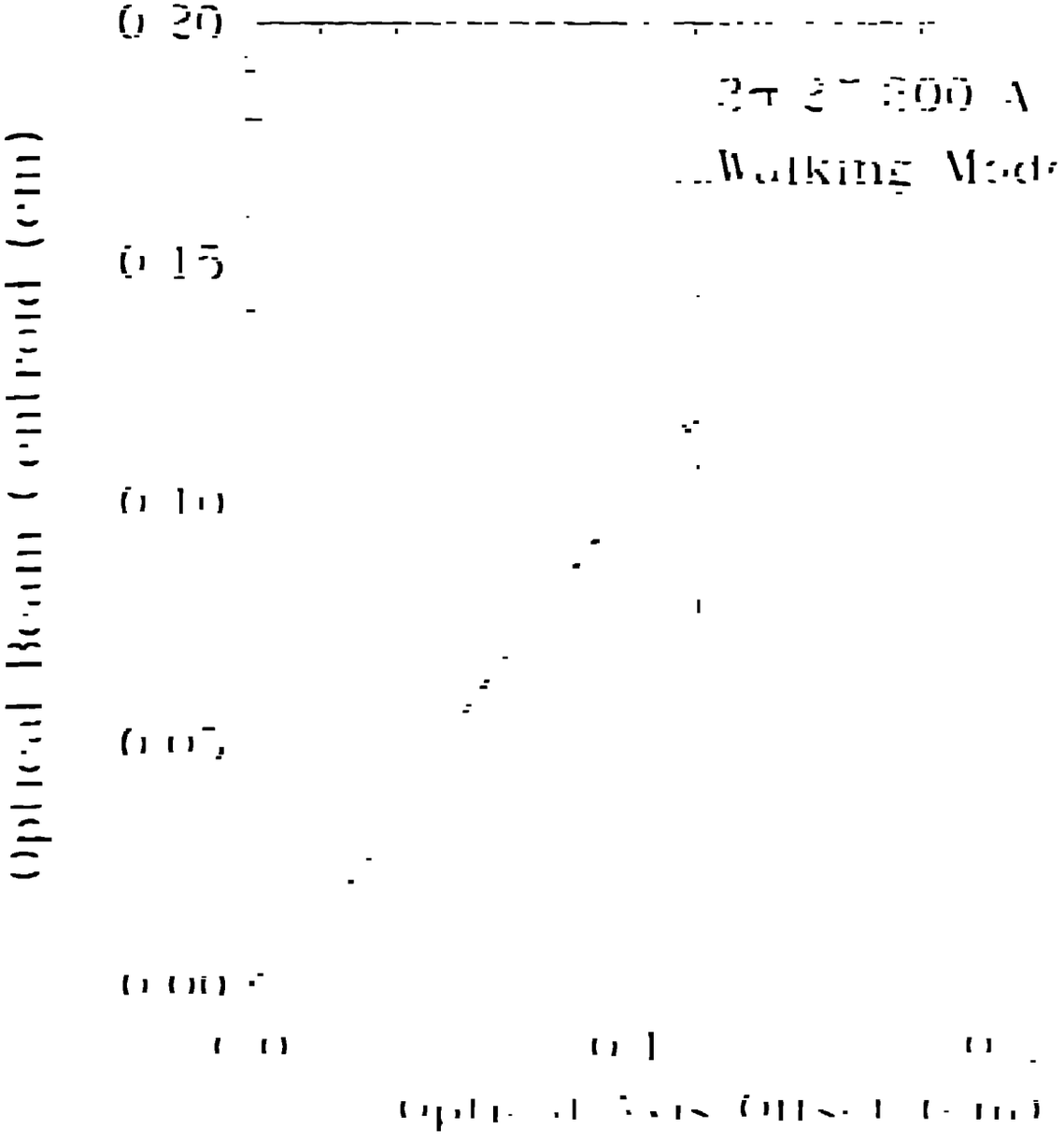
Walking Mode
0.20
0.15
0.10
0.05
0.00
0.0
0.1